Rev. Mexicana Astron. Astrof., 13, 57-64 (1986)

CORRELATIONS BETWEEN OBSERVATIONAL PARAMETERS OF THE CONDENSATIONS IN HERBIG–HARO OBJECT 2

J. Cantó and L.F. Rodríguez

Instituto de Astronomía
Universidad Nacional Autónoma de México

Received 1986 February 26

RESUMEN

En este trabajo se presentan correlaciones observacionales entre la intensidad de la línea Hα y la densidad electrónica deducida de las líneas rojas de [S II], con la velocidad espacial en las partes más brillantes de las condensaciones de HH2. Se muestra también, que existe una correlación entre el tamaño de la condensación y su velocidad. Estas correlaciones son en el sentido: intensidad de Hα $\propto V^2$; densidad electrónica $\propto V$ y tamaño $\propto V$. Las primeras dos correlaciones se pueden explicar bajo un modelo en el cual, la parte más brillante de cada condensación representa una onda de choque plano–paralela moviéndose con una velocidad igual a la velocidad observada de la condensación: todas las ondas moviéndose en el mismo medio. Estas ondas de choque planas se interpretan como las cabezas de las ondas de choque en forma de arco que se forman cuando condensaciones de alta velocidad se mueven en el medio interestelar. La última de las correlaciones podría también explicarse con el mismo modelo, puesto que la zona emisora de una onda de choque en forma de arco (para un tamaño de condensación fijo) aumenta linealmente con la velocidad de la onda.

ABSTRACT

In this paper we present empirical correlations between the Hα line intensity and [S II] electron density with the total spatial velocity for the brightest part of individual knots in HH2. Also we show that there is a correlation between the size of a knot and its total velocity. These correlations are in the sense: Hα intensity $\propto V^2$; electron density $\propto V$ and size $\propto V$. The first two correlations fit with a model in which the brightest part of each knot represents a single plane-parallel shock wave with velocity equal to the spatial velocity of the knot, all moving into the same medium. These plane-parallel shocks are interpreted as the heads of bow shocks formed as high-velocity clumps plunge into the interstellar medium. The last correlation may also be explained since the extent of the emitting zone of a bow shock (for a given clump size) increases linearly with velocity.

Key words: HERBIG-HARO OBJECTS — SHOCK WAVES

I. INTRODUCTION

Since the time of their discovery by Haro (1950) and Herbig (1951), one of the most important aspects of the Herbig-Haro object phenomenon has been their excitation mechanism. The pioneering work of Böhm (1956), Osterbrock (1958) and Haro and Minkowski (1960) firmly established that HH-objects could not be the result of simple photoionization from a central source. In 1975, Schwartz (1975) drew attention to the great similarities between the optical spectra of these objects and the SNR N49 in the LMC. This fact pointed to the interpretation of HH-objects as the cooling region of interstellar shock waves of moderate velocity. Fitting with this interpretation there were the highly supersonic radial velocities exhibited by most objects. Years later, Raymond (1976, 1979), Dopita (1978) and Shull and McKee (1979) performed detailed calculations of the emission spectra of plane-parallel shock waves in steady state and showed that the mean observed features in the optical spectra of HH-objects could be reproduced with preshock densities of ~ 100 cm^{-3} and shock velocities of ~ 100 km s^{-1}.

A real challenge for the interpretation of HH-objects as simple (plane-parallel and steady state) shock waves came with the detection of ultraviolet emission from these objects (see Böhm 1983 and references therein). The *UV* spectra of HH1 and 2 show emission lines of highly ionized ions (C III and IV, O III and IV and Si III and IV) whose strength can not be reproduced with the same shock model which accounts for the optical spectra. A much larger (~ 200 km s^{-1}) shock velocity is suggested from the high excitation *UV* emission lines. A plausible explanation for this apparent disagreement is that HH-objects represent bow shocks which are the result of the interaction of dense clumps of material against a less dense supersonic stream (Schwartz 1978; Hartmann and Raymond 1984). In this case, the ob-

served spectrum would be the blend of the spectra of a continuum of shocks with velocities ranging from the velocity of the impinging stream (the maximum velocity) down to zero. Further evidence for a bow geometry in HH-objects is given by the fact that the predicted line shapes are similar to those observed (Choe, Böhm, and Solf 1984).

Hartmann and Raymond (1984) have presented detailed calculations of the spectra of bow shocks with maximum velocities in the range 160-300 km s^{-1}. They found that the line widths and the optical and *UV* spectra of HH1 and HH2 are in reasonable agreement with calculations for maximum shock velocities of $\sim$ 200 km s^{-1}. Since such velocities are comparable to the spatial (radial plus transverse) velocities of the knots in HH1 and HH2, it was concluded that HH-objects represent high velocity dense clumps shocking with less dense interstellar material.

In this paper we present further evidence in this sense. Our study is restricted to HH2 for which spectroscopic, radial and proper motion information for individual condensations is available. In §II we discuss the data and present the correlations between the electron density, Hα line intensity and size of condensations with their spatial velocity. In §III we interpret these correlations in the framework of the shock wave theory, while in §IV we give our conclusions.

II. DISCUSSION OF THE DATA

Most of the spectrophotometric observations of HH-objects available in the literature have been performed in such a way that the slit or the diaphragm used included entire objects or entire knots within one object. The spectra obtained in this way are then likely to correspond to the entire bow shock, and thus their interpretation in terms of simple plane-parallel, steady state shock waves is inadequate. They should be interpreted in terms of bow shock models (Hartmann and Raymond 1984).

In contrast, the study by Schwartz (1978) of individual knots in HH2 was done using a slit of only 1″, which is substantially smaller than the apparent size of knots in this object. Also, the length and width of the PDS slit was chosen in such a way that it was much less than the length of a given emission knot on the plate. Furthermore, traces were made parallel to the dispersion through the central portion of each line. These three facts suggest that the emission line intensities reported by Schwartz correspond (mainly) to the central, brightest parts of each knot, that is, that they correspond to the central parts of the bow shocks. In this case, we expect the line spectra to be easier to interpret, since the central part of a bow shock can roughly be approximated as plane-parallel. The velocity of the shock is the velocity of the impinging stream.

Having this idea in mind, we adopt the relative line intensities reported by Schwartz (1978) as our basic set of data. In Table 1 we give the intensity of the Hα line (in arbitrary units) and the electron density dependent intensity ratio of the [S II] red lines. Also we list in this table the corresponding electron densities for $T = 10^4$ K.

First we investigate if there is any correlation between the Hα intensity and the electron density with the total (spatial) velocity of the knots. For this, we use the radial velocities also reported by Schwartz (1978) and the tan-

TABLE 1

OBSERVED AND DERIVED PARAMETERS FOR INDIVIDUAL KNOTS IN HH2

Condensation	V_r[1] (km s^{-1})	ΔV_r[2] (km s^{-1})	ΔV_T[3] (km s^{-1})	V_{TOT}[5] (km s^{-1})	I (6717)/I(6731)[6]	log n_e[8] (cm^{-3})	I (Hα)[10]	D[11] (arcsec)
A	21 ± 4	3 ± 4	153:[4]	153:	0.67	3.26 ± 0.17	141	3.3 ± 0.3
B	13 ± 6	− 5 ± 6	100 ± 13	100 ± 13	0.72	3.14 ± 0.15	112	2.0 ± 0.1
C	31 ± 5	13 ± 5	294 ± 24	294 ± 24	0.96[7]	2.70 ± 0.18[9]	64	1.3 ± 0.1
D	...	...	85 ± 22	...	...	...	...	1.4 ± 0.2
E	39 ± 6	21 ± 6	61 ± 22	65 ± 22	0.77	3.04 ± 0.15	52	1.6 ± 0.2
G	− 2 ± 8	− 20 ± 8	153 ± 9	154 ± 9	0.62	3.40 ± 0.16	285	2.8 ± 0.2
H	13 ± 2	− 5 ± 2	241 ± 13	241 ± 13	0.53	3.66 ± 0.18	652	4.4 ± 0.2
I	...	...	?38 ± 48	...	...	...	...	1.0 ± 0.1
L	11 ± 3	− 7 ± 3	...	...	0.77	3.76 ± 0.18	26	1.6 ± 0.2

1. Heliocentric radial velocity derived from the red lines of [O I], [N II], Hα and [S II] (Schwartz 1978).
2. Radial velocity with respect to the cloud: $\Delta V_r = V_r$ (HH) − V_r (cloud); V_r (cloud) = + 18 km s^{-1} (Schwartz 1978).
3. Tangential velocity with respect to the cloud (Herbig and Jones 1981). Adopted distance 460 pc.
4. In the late 1950's a new nucleus (A′) appears about 1″ north of A. This new nucleus has a tangential velocity of 46.5 km s^{-1}
5. Total spatial velocity with respect to the cloud: $V_{TOT} = (\Delta V_r^2 + \Delta V_T^2)^{1/2}$.
6. Ratio of relative intensities obtained through a 1″ slit and uncorrected for extinction (Schwartz 1978).
7. Relative intensities between lines in a given knot are in agreement ($\sim$ 20%) with data reported by other authors (Dopita 1978; Böhm, Siegmund and Schwartz 1976). However for this condensation Dopita (1978) reports $\sim$ 0.50.
8. Electron density derived from the [S II] ratio for $T = 10^4$ K, using the transition probabilities of Mendoza and Zeippen (1982) and the reaction-rate parameters of Pradhan (1978).
9. For the ratio 0.5 given by Dopita (1978), log $n_e = 3.76 \pm 0.18$.
10. Relative intensities obtained through a 1″ slit and uncorrected for extinction in arbitrary units (Schwartz 1978).
11. Angular diameter estimated from the 1980 (Figure 2) of Herbig and Jones (1981). Errors are derived from three independent measurements.

gential velocities corresponding to the proper motions measured by Herbig and Jones (1981). We adopt a distance of 460 pc. The velocities of each knot are also given in Table 1.

Figure 1*a* is a plot of the Hα line intensities and the [S II] electron densities of each knot against their spatial velocities. Clearly both quantities are *directly* correlated with velocity. The electron density increases with velocity, approximately as $\propto V$; while the Hα line intensity increases with velocity as $\propto V^2$. These correlations will be discussed in the next section. Here we just point out that these correlations are *opposite* to the correlations that Schwartz and Dopita (1980) propose to exist among a large sample of HH-objects. These authors present plots of the modulus of the radial velocity and the excitation state within the object (estimated by the ratio [O III] λ5007/[O I] λ6300) against the modulus of the radial velocity and the [S II] electron density. In their view, the lack of HH-objects with high radial velocities showing high excitation or having high electron density indicates that the velocity of the shock wave and the velocity of the emitting material are *inversely* related. As we will see in the next section, this conclusion is exactly the opposite to that indicated by Figure 1.

Another empirical correlation which is likely to give us information on the origin of HH-objects is that shown in Figure 2. There, we plot the apparent angular size of each condensation (estimated from the 1980 photograph of Herbig and Jones (1981); their Figure 2) against its spatial velocity. Again it appears to be a direct correlation between them, *vis.*, (angular size) $\propto V$. This correlation will also be discussed in the next section.

III. DISCUSSION OF THE MODEL

As we will see the correlations between the Hα line intensity and the [S II] electron density with the total (spatial) velocity of the condensations can be understood in a model in which each condensation of HH2

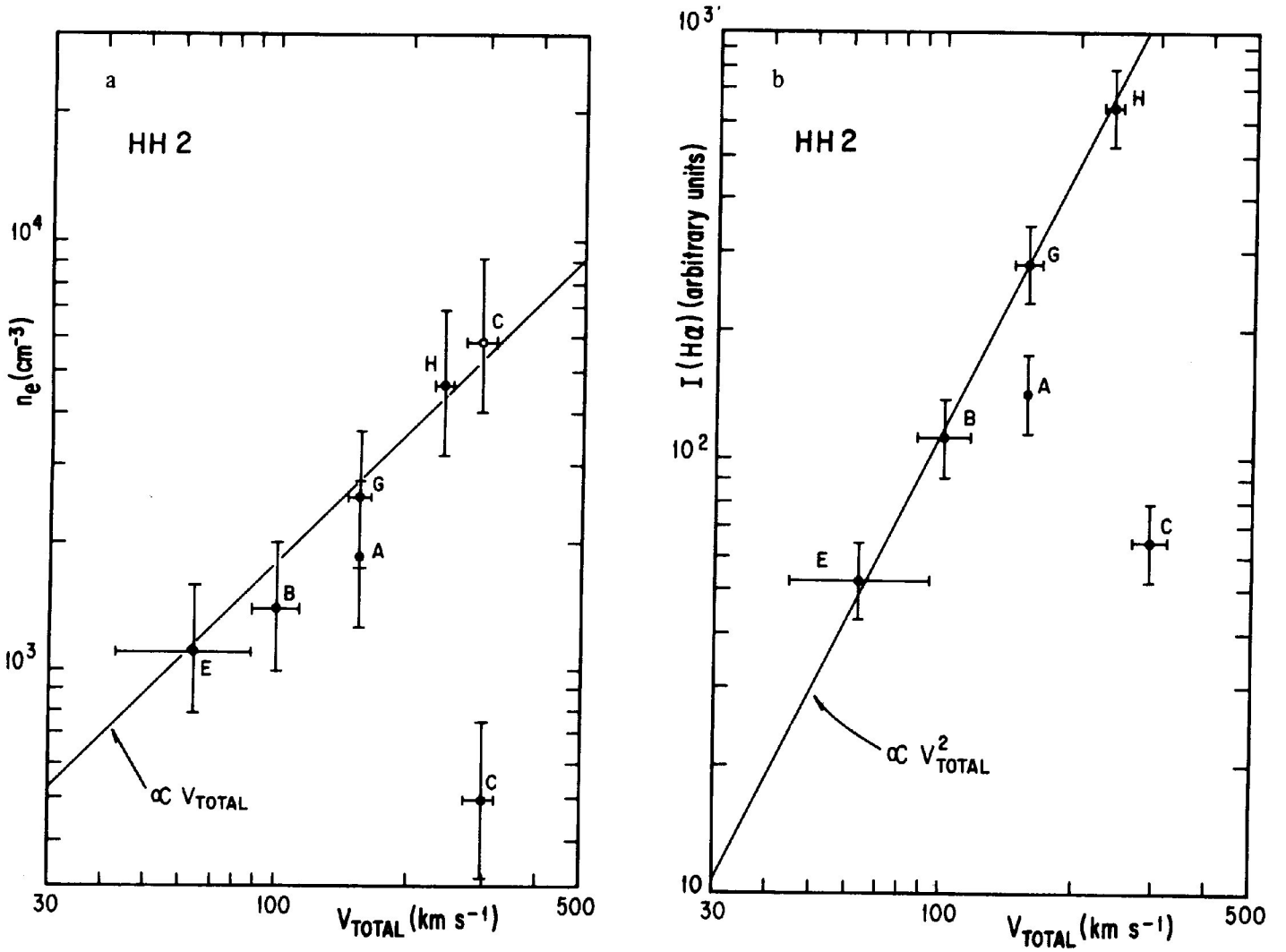

Fig. 1. Correlations between (a) electron density, and (b) Hα line intensity with their spatial velocity for the brightest parts of individual condensations in HH2. The data and the sources of information are given in Table 1. The open circle in (a) represents the measurement of Dopita (1978).

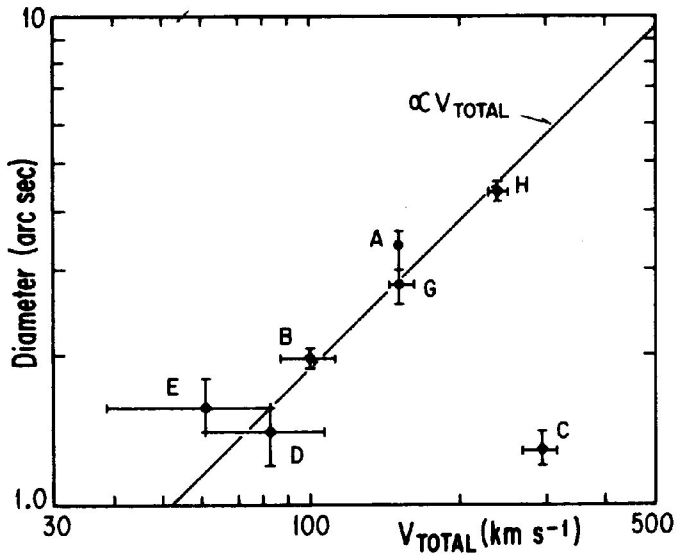

Fig. 2. Correlation between the angular diameter of condensations in HH2 with their spatial velocity. The broken line represents the predicted behaviour (Rozyczka and Tenorio-Tagle 1985) if the condensations represents bow shocks produced by clumps of similar sizes but different velocities.

(actually its brightest part) represents a single plane-parallel steady shock wave moving with a velocity equal to its spatial velocity. All condensations are moving in the same medium.

In Appendix I we consider a strong, plane-parallel, steady state shock wave moving with velocity v_0 into a medium with hydrogen density n_0, thermal pressure P_0 and magnetic field intensity B_0 parallel to the shock front. There, we show that the electron density that would be deduced from the [S II] line ratio in the case of a non-negligible magnetic field is,

$$\left[\frac{n_e}{\text{cm}^{-3}}\right] = 3.82 \times 10^3 \left[\frac{n_0}{100\ \text{cm}^{-3}}\right]^{3/2} \left[\frac{B_0}{10\ \mu\text{G}}\right]^{-1} \left[\frac{v_0}{100\ \text{km s}^{-1}}\right] \quad (1)$$

We notice that Eq. (1) gives a linear dependence on the shock velocity. Recalling that the observed dependence of the electron density with the total velocity for condensations in HH2 is also linear, it is natural to propose a model in which the brightest part of each condensation represents a single plane-parallel, steady shock, with velocity equal to the spatial velocity of the condensation and all moving into a same medium with a non-negligible magnetic field.

This model can be tested by comparing the observed correlation between the intensity of the Hα line and velocity ($\propto V^2$; §II) with that predicted by the model. For this we use the detailed calculations of the emission by plane-parallel, steady state shock waves by Raymond (1976, 1979) and Shull and McKee (1979). Figure 3 shows the Hα line intensity (erg cm^{-2} s^{-1} str^{-1}) as a function of the shock velocity for several models with the same $n_0 = 10$ cm^{-3}, $B_0 = 1\mu$G and abundances (cosmical), as given by Raymond (1976) and Shull and Mc Kee (1979). The two sets of models show an increase of the Hα line intensity with velocity approximately as $\propto V^2$ (except for $V \lesssim 70$ km s^{-1} in Shull and McKee's models). Indeed, the straight line on Figure 3 represents a fit to Raymond's models of the form

$$\left[\frac{I(\text{H}\alpha)}{\text{erg cm}^{-2}\ \text{s}^{-1}\ \text{str}^{-1}}\right] = 1.66 \times 10^{-9} \left[\frac{V_s}{\text{km s}^{-1}}\right]^2 \quad (2)$$

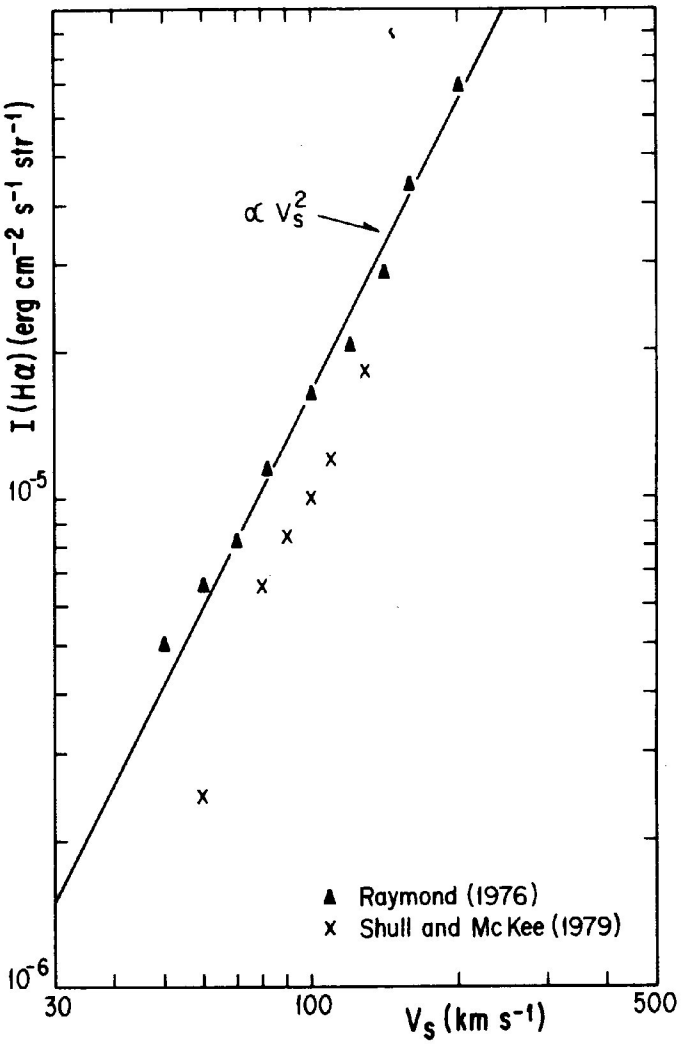

Fig. 3. Hα line intensity predicted by shock models as a function of shock velocity. The pre-shock hydrogen density and magnetic field strength are 10 cm^{-3} and 1 μG, respectively, for all models. The line represents a fit to Raymond's models.

A similar fit can be obtained for Shull and McKee's models for shock velocities $V \gtrsim 70$ km s^{-1}, although the scale coefficient is ~ 1.6 times lower than the value given in Eq. (2). The differences in the scale factor and in the behavior of the Hα intensity for $V \lesssim 70$ km s^{-1} between the two sets of models is likely to be the result of different assumptions regarding the pre-shock ionization. Raymond assumes complete pre-ionization of hydrogen, while Shull and McKee calculate it in a self-consistent manner by considering the flux of ionizing photons produced in the wave and travelling upstream.

In any case, it appears that in the range of velocities considered in this work, the Hα line intensity is expected to increase as the square of the shock velocity. This is the same behavior we observe in the condensations of HH2 (Figure 1*b*), if we identify the spatial velocity of each condensation with the velocity of the shock that gives rise to the Hα emission. Thus, our model of individual shock waves moving with a velocity equal to the spatial velocity of the emitting material is further supported.

Adopting this model we now proceed to estimate the parameters (n_0 and B_0) of the pre-shock medium. For this, we first compare Eq. (1) with the fit in the $n_e - V_{TOT}$ plot of Figure 1*a*.

$$\left[\frac{n_e}{\text{cm}^{-3}}\right] = 1.78 \times 10^3 \left[\frac{V_{TOT}}{100 \text{ km s}^{-1}}\right]$$

to obtain

$$\left[\frac{n_0}{100 \text{ cm}^{-3}}\right]^{3/2} \left[\frac{B_0}{10\ \mu\text{G}}\right]^{-1} = 0.47 \qquad (3)$$

where we have identified the total velocity of the knots with the shock velocity.

This result can be combined with the absolute fluxes of the Hα line for individual condensations in HH2 and the shock models to estimate n_0 and B_0 separately. According to Brugel, Böhm, and Mannery (1981), the absolute flux in the Hα line above the Earth's atmosphere corrected for extinction for condensation H of HH2 is $\sim 8.7 \times 10^{-13}$ erg cm^{-2} s^{-1}. Adopting for this condensation an angular diameter of 4.4″ (Table 1), an intensity of $\sim 2.5 \times 10^{-3}$ erg cm^{-2} s^{-1} str^{-1} in this line is derived.

As we showed above (see also Raymond 1976), the detailed shock calculations indicate $I(H\alpha) \propto V_s^2$. Also, from these calculations we found that I(Hα) seems to be directly proportional to the pre-shock density, n_0, and nearly insensitive to B_0. The models presented in Figure 3 were calculated with $n_0 = 10$ cm^{-3}. Thus the Hα line intensity as a function of n_0 and V_s may be written as

$$\left[\frac{I(H\alpha)}{\text{erg cm}^{-2}\text{ s}^{-1}\text{ str}^{-1}}\right] \cong 1.66 \times 10^{-8} \left[\frac{n_0}{100 \text{ cm}^{-3}}\right] \left[\frac{V_s}{\text{km s}^{-1}}\right]^2 \qquad (4)$$

where we have used Eq. (2). Taking for HH2-H, $V_s \cong 240$ km s^{-1} (the total spatial velocity; Table 1) and $I(H\alpha) \cong 2.5 \times 10^{-3}$ erg cm^{-2} s^{-1} str^{-1} (see above), Eq. (4) gives,

$$n_0 \cong 260 \text{ cm}^{-3}$$

a reasonable value for the outer parts of molecular clouds.

Using this estimate for the pre-shock hydrogen density in Eq. (3), one finds,

$$B_0 \cong 89\ \mu\text{G}$$

as a rough estimate. We can see, however, that this estimate for the pre-shock magnetic field is consistent with the limits we derive from the relation, given by Brown and Chong-An Chang (1983), between the magnetic field strength and the gas density in interstellar clouds, *vis.*,

$$\left[\frac{B}{\mu\text{G}}\right] = 3.8^{+17}_{-3.1} \left[\frac{n}{\text{cm}^{-3}}\right]^{0.44}$$

when it is extrapoled to dense molecular clouds. For $n \sim 260$ cm^{-3} we obtain $B = 0.8 - 240\ \mu$G.

Finally, we will discuss the correlations between the diameter of the knots and their spatial velocity (Figure 2). The solid line in Figure 2 represents the fit,

$$\left[\frac{d}{\text{arcsec}}\right] = 1.91 \times 10^{-2} \left[\frac{V_{TOT}}{\text{km s}^{-1}}\right] \qquad (5)$$

This correlation may also be explained in a model in which each condensation represents a bow shock, all moving into the same medium. Rozyczka and Tenorio-Tagle (1985) have recently investigated the properties of bow shocks which are formed around dense clumps impinged by a supersonic stream. In particular, they show (their Figure 4) maps of the total (frequency-integrated) emission of the shock for velocities in the range 25–400 km s^{-1}. For velocities between 25 and 200 km s^{-1}, it is found that the bulk of the optical

emission comes from the head of the bow shock, with the emission dropping very rapidly towards the lee side of the clump. The extent of the emitting zone perpendicular to the flow direction is always similar to the clump radius and does not change appreciably with velocity. The length (measured along the flow direction), however, is an increasing function of velocity. It is clear that the predicted behaviour is quite similar to that observed, if each condensation represents a bow shock produced by clumps of similar size but moving at different velocities.

Nevertheless, there is a problem with this interpretation of the empirical behaviour. The condensations in HH2 are approximately round, while the Rozyczka and Tenorio-Tagle (1985) modeling would imply emitting zones elongated along the direction of motion. We conclude that this last correlation (diameter $\propto$ spatial velocities) can be accounted for only partially.

IV. CONCLUSIONS

Our main conclusions can be summarized as follows:

1) The Hα line intensity and [S II] electron density from the central brightest part of individual knots in HH2 show direct correlations with their total spatial velocity. The size for individual knots also increases with the total velocity. More specifically:

a) Hα line intensity $\propto V_{TOTAL}^2$
b) Electron density $\propto V_{TOTAL}$
c) Angular diameter $\propto V_{TOTAL}$

2) Correlations (a) and (b) can be interpreted in a model in which the brightest part of each condensation represents a single, plane-parallel shock wave with velocity equal to the total spatial velocity of the condensation. These plane-parallel shocks are interpreted as the heads of bow shocks formed as high-velocity clumps plunge into the interstellar medium.

3) The estimated values for the hydrogen density and magnetic field of the medium through which the clumps are moving at ~ 260 cm^{-3} and ~ 90 μG respectively. These values are consistent with those expected to prevail in the outer parts of molecular clouds.

4) Correlation (c) may be explained partially in terms of bow shocks if the clumps have similar sizes but are moving at different velocities.

5) These results suggest that, at least for HH2, we can favor the model of the "interstellar bullets" (dense clumps moving supersonically in a tenuous ambient medium, Norman and Silk 1979; Rodríguez *et al.* 1980) as opposed to the model of "cloudlets" being shocked by a stellar wind (Schwartz 1978). However, for other HH objects the results of Schwartz and Dopita (1980) favor the "cloudlet" model. It is obvious that further research is needed before this basic characteristic of the kinematics of HH objects can be determined.

This work was partially supported by a grant from *CONACYT* (México), No. PCCBBNA-022688. This is Contribution No. 194 of Instituto de Astronomía, UNAM.

REFERENCES

Böhm, K.H. 1956, *Ap. J.*, **123**, 379.
Böhm, K.H. 1983, *Rev. Mexicana Astron. Astrof.*, 7, 55.
Böhm, K.H., Siegmund, W.A., and Schwartz, R.D. 1976, *Ap. J.*, **203**, 399.
Brown, R.L. and Chong-An Chang, 1983, *Ap. J.*, **264**, 134.
Brugel, E.W., Böhm, K.H. and Mannery, E. 1981, *Ap. J. Suppl.*, **47**, 117.
Choe, S.U., Böhm, K.H., and Solf, J. 1984, *Ap. J.*, **288**, 338.
Dopita, M.A. 1978, *Ap. J. Suppl.*, **37**, 117.
Haro, G. 1950, *Ap. J.*, **55**, 72.
Haro, G. and Minkowski, R. 1960, *Ap. J.*, **65**, 490.
Hartmann, L. and Raymond, J.C. 1984, *Ap. J.*, **276**, 560.
Herbig, G.H. 1951, *Ap. J.*, **113**, 697.
Herbig, G.H. and Jones, B.F. 1981, *A.J.*, **86**, 1232.
Mendoza, C. and Zeippen, C.J. 1982, *M.N.R.A.S.*, **199**, 1025.
Norman, C. and Silk, J. 1979, *Ap. J.*, **228**, 197.
Osterbrock, D.E. 1958, *P.A.S.P.*, **70**, 399.
Pradhan, A.K. 1978, *M.N.R.A.S.*, **183**, 89p.
Raymond, J.C. 1976, Ph.D. Thesis, University of Wisconsin Madison.
Raymond, J.C. 1979, *Ap. J. Suppl.*, **39**, 1.
Rodríguez, L.F., Moran, J.M., Ho, P.T.P., and Gottlieb, E.W. 1980, *Ap. J.*, **235**, 845.
Rozyczka, M. and Tenorio-Tagle, G. 1985, *Astr. and Ap.*, **147**, 220.
Schwartz, R.D. 1975, *Ap. J.*, **195**, 631.
Schwartz, R.D. 1978, *Ap. J.*, **223**, 884.
Schwartz, R.D. and Dopita, M. 1980, *Ap. J.*, **236**, 543.
Shull, J.M. and McKee, C.F. 1979, *Ap. J.*, **220**, 525.

APPENDIX I

ELECTRON DENSITY–SHOCK VELOCITY RELATION IN ISOTHERMAL SHOCKS

Consider a plane-parallel steady flow with mass density ρ_0, thermal pressure P_0, magnetic field B_0 perpendicular to the flow, and velocity v_0 with respect to the shock front. Conservation of mass and momentum gives,

$$\rho v = \rho_0 v_0 \tag{A1}$$

$$P + \rho v^2 + \frac{B^2}{8\pi} = P_0 + \rho_0 v_0^2 + \frac{B_0^2}{8\pi} \tag{A2}$$

where P, ρ, v and B are the values of the variables at any point in the relaxation region behind the shock front. If the magnetic field is assumed to be frozen-in, then,

$$\frac{B}{\rho} = \frac{B_0}{\rho_0} \tag{A3}$$

The pressure and mass density are related by $P = \rho c^2$; where c is the sound speed.

Let us consider that region behind the shock where the temperature has reached its pre-shock value. There, $c = c_0$ and the substitution of (A1) and (A3) in (A2) gives,

$$\frac{1}{2}v_{A_0}^2\left[\left(\frac{\rho}{\rho_0}\right)^2 - 1\right] + c_0^2\left[\left(\frac{\rho}{\rho_0}\right) - 1\right] - v_0^2\left[\frac{(\rho/\rho_0) - 1}{(\rho/\rho_0)}\right] = 0 \qquad \text{(A4)}$$

where $v_{A_0} \equiv (B_0^2/4\pi\rho_0)^{1/2}$ is the Alfvén speed in the unshocked stream. Since we expect $(\rho/\rho_0) \neq 1$, then Eq. (A4) simplifies to

$$\frac{1}{2}v_{A_0}^2\left(\frac{\rho}{\rho_0}\right)^2 + \left[\frac{1}{2}v_{A_0}^2 + c_0^2\right]\left(\frac{\rho}{\rho_0}\right) - v_0^2 = 0 \qquad \text{(A5)}$$

whose solution is,

$$\left(\frac{\rho}{\rho_0}\right) = \sqrt{\left(\frac{1}{2} + \frac{c_0^2}{v_{A_0}^2}\right)^2 + 2\left(\frac{v_0^2}{v_{A_0}^2}\right)} - \left(\frac{1}{2} + \frac{c_0^2}{v_{A_0}^2}\right). \qquad \text{(A6)}$$

Two limiting cases follow. For a negligible magnetic field or a small compression factor (ρ/ρ_0), Eq. (A6) reduces to the familiar result,

$$\left(\frac{\rho}{\rho_0}\right) \cong \left(\frac{v_0}{c_0}\right)^2 \qquad \text{(A7)}$$

which indicates that the compression across an isothermal shock increases as the square of the velocity of the shock.

On the other hand, for a non-negligible magnetic field and/or a strong compression factor, Eq. (A6) yields,

$$\left(\frac{\rho}{\rho_0}\right) \cong 2^{1/2}\left(\frac{v_0}{v_{A_0}}\right) \qquad \text{(A8)}$$

which predicts a linear increase of the compression with the shock velocity.

The critical value for the compression factor (for given pre-shock magnetic field and density) which separates the two regimes can be estimated by the condition,

$$\frac{1}{2}v_{A_0}^2\left(\frac{\rho}{\rho_0}\right)^2 \cong \left(\frac{1}{2}v_{A_0}^2 + c_0^2\right)\frac{\rho}{\rho_0}$$

which yields,

$$\left(\frac{\rho}{\rho_0}\right) \cong 1 + 2\left(\frac{c_0}{v_{A_0}}\right)^2 . \qquad \text{(A9)}$$

This compression factor corresponds to a shock velocity

$$v_0 \cong v_{A_0}\left[1 + 2\left(\frac{c_0}{v_{A_0}}\right)^2\right]. \qquad \text{(A10)}$$

Numerically, the pre-shock Alfvén and sound speeds are given by,

$$\frac{v_{A_0}}{\text{km s}^{-1}} = 1.85\left(\frac{B_0}{10\,\mu\text{G}}\right)\left(\frac{n_0}{100\text{ cm}^{-3}}\right)^{-1/2} \qquad \text{(A11)}$$

and

$$\left(\frac{c_0}{\text{km s}^{-1}}\right) = 7.68\left(\frac{T_0}{10^4\text{K}}\right)^{1/2}(1.1 + \xi_0)^{1/2}$$

where T_0 and n_0 denote the pre-shock temperature and density of hydrogen nuclei, respectively. $\xi_0 (\equiv n_{e_0}/n_0)$ is the pre-shock hydrogen ionization (helium is assumed to remain neutral). A helium to hydrogen particle ratio of 0.1 has been assumed.

Before we proceed to estimate the electron density in the post-shock region, we should mention that Eq. (A6) and thus all the results and conclusions derived from it are also approximately correct for strong shocks even if the isothermal condition is not met. That is, Eq. (A6) gives the density of mass in that part of the cooling region where the temperature equals the pre-shock temperature. However, Eq. (A6) can also be used to estimate the mass density at any point in the cooling region, provided we substitute the pre-shock sound speed c_0 by the sound speed of the region under consideration.

Let n_e and ξ be the electron density and hydrogen ionization ratio in the post-shock region. If helium is also assumed to be neutral in this region,

$$\left(\frac{\rho}{\rho_0}\right) = \frac{n_e}{n_0\xi}$$

and, from Eq. (A6),

$$n_e = \xi n_0 \left[\sqrt{\left(\frac{1}{2}+\frac{c_0^2}{v_{A_0}^2}\right)^2 + 2\left(\frac{v_0}{v_{A_0}}\right)^2} - \left(\frac{1}{2}+\frac{c_0^2}{v_{A_0}^2}\right)^2 \right] \qquad \text{(A12)}$$

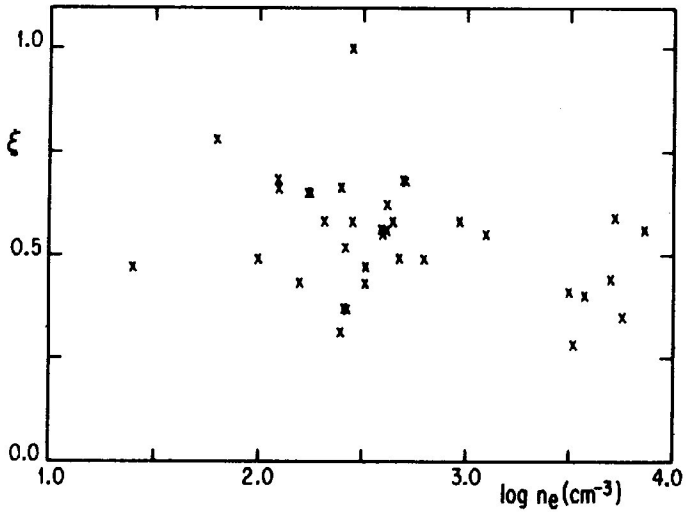

Fig. A1. Hydrogen ionization ratio required by Eq. (A12) to match the electron density deduced from the [S II] lines for each model given by Raymond (1976). Notice that despite the very different shock parameters assumed for each model, the ionization ratio can be taken ~ 0.5, within a factor of two.

in the region where the shocked flow has cooled down to a temperature equal to the pre-shock temperature.

The hydrogen ionization ratio in this region can be estimated by comparing Eq. (A12) with the results of the detailed calculations of the structure of shock waves as reported by Raymond (1976). For this, we use the forbidden red lines of [S II] whose ratio is sensitive to the electron density. The [S II] lines are expected to be emitted mainly in that part of the cooling region where $T \sim 10^4$ K. Figure (A1) shows a plot of the hydrogen ionization ratio required by Eq. (A12) to match the electron density deduced from the [S II] lines for each model given by Raymond (1976). It follows from this figure that Eq. (A12) with $\xi = 0.5$ is able to reproduce Raymond's results within a factor of two.

Finally, we give the numerical expression for the electron density that would be deduced from the [S II] lines ratio in the limiting case of a non-negligible magnetic field and/or a strong compression factor (Eq. (A8)). This is,

$$\left(\frac{n_e}{\text{cm}^{-3}}\right) = 3.82 \times 10^3 \left(\frac{n_0}{100\ \text{cm}^{-3}}\right)^{3/2} \left(\frac{B_0}{10\ \mu\text{G}}\right)^{-1} \left(\frac{V_0}{100\ \text{km s}^{-1}}\right) \qquad \text{(A13)}$$

where we have adopted $\xi = 0.5$.

Jorge Cantó and Luis F. Rodríguez: Instituto de Astronomía, UNAM, Apartado Postal 70-264, 04510 México, D.F., México.